JOURNAL OF VIROLOGY, Oct. 2000, p. 8867–8875 Vol. 74, No. 19
0022-538X/00/$04.00+0

Substitutions at the Putative Receptor-Binding Site of an Encephalitic Flavivirus Alter Virulence and Host Cell Tropism and Reveal a Role for Glycosaminoglycans in Entry

EVA LEE AND MARIO LOBIGS*

Division of Immunology and Cell Biology, John Curtin School of Medical Research, Australian National University, Australian Capital Territory, Australia

Received 3 May 2000/Accepted 10 July 2000

The flavivirus receptor-binding domain has been putatively assigned to a hydrophilic region (FG loop) in the envelope (E) protein. In some flaviviruses this domain harbors the integrin-binding motif Arg-Gly-Asp (RGD). One of us has shown earlier that host cell adaptation of Murray Valley encephalitis virus (MVE) can result in the selection of attenuated variants altered at E protein residue Asp_{390}, which is part of an RGD motif. Here, a full-length, infectious cDNA clone of MVE was constructed and employed to systematically investigate the impact of single amino acid changes at Asp_{390} on cell tropism, virus entry, and virulence. Each of 10 different E protein 390 mutants was viable. Three mutants (Gly_{390}, Ala_{390}, and His_{390}) showed pronounced differences from an infectious clone-derived control virus in growth in mammalian and mosquito cells. The altered cell tropism correlated with (i) a difference in entry kinetics, (ii) an increased dependence on glycosaminoglycans (determined by inhibition of virus infectivity by heparin) for attachment of the three mutants to different mammalian cells, and (iii) the loss of virulence in mice. These results confirm a functional role of the FG loop in the flavivirus E protein in virus entry and suggest that encephalitic flaviviruses can enter cells via attachment to glycosaminoglycans. However, it appears that additional cell surface molecules are also used as receptors by natural isolates of MVE and that the increased dependence on glycosaminoglycans for entry results in the loss of neuroinvasiveness.

Virus attachment to the host cell is the first stage of the virus replication cycle. It requires the molecular interaction between the virion surface and a host cell receptor and is often the basis for viral species and tissue tropisms as well as virulence properties. The cellular receptors for some viruses have been defined and reveal diverse strategies for virus attachment, ranging from binding to specific cell surface proteins to attachment via widely distributed carbohydrate moieties, such as sialic acid and heparan sulfate (for a review, see reference 48). For a large number of viruses, however, specific host cell receptors have not been identified. The use of multiple receptors on individual or different cells could be one reason for this lack of knowledge. This scenario has been proposed for the attachment of flaviviruses (35), a genus of approximately 70 mainly arthropod-borne, enveloped RNA viruses. Most flaviviruses replicate in vertebrate and arthropod cells and exhibit a wide species and tissue tropism. Numerous candidate receptor proteins with a molecular mass of 40 to 80 kDa have been found to associate with flaviviruses in binding assays (19, 22, 27, 36, 44). Furthermore, an important role of heparan sulfate has also been demonstrated for the attachment of dengue-2 virus to vertebrate cells (7). Interestingly, cell surface glycosaminoglycans (GAGs) are exploited as attachment molecules by other viruses in a process thought to concentrate virus particles at the cell surface for subsequent binding to high-affinity receptors (for a review, see reference 2). No experimental evidence on the use or nature of a high-affinity receptor for any of the flaviviruses exists at present.

* Corresponding author. Mailing address: Division of Immunology and Cell Biology, John Curtin School of Medical Research, Australian National University, P.O. Box 334, Canberra, ACT 2601, Australia. Phone: 61-2-62494048. Fax: 61-2-62492595. E-mail: Mario.Lobigs@anu.edu.au.

Flavivirus attachment and entry are mediated by the envelope (E) protein (~50 kDa), the major glycoprotein on the flavivirus particle (for reviews, see references 6 and 33). The E protein forms an oligomer with the small membrane (M) protein (~8 kDa) and constitutes most of the accessible virion surface; this is reflected in the dominance of the E protein as target antigen for virus-neutralizing and protective antibodies (33). The definition of the crystal structure of the ectodomain of the E protein of the flavivirus tick-borne encephalitis virus (TBE) (37), in combination with phenotypic analyses of E protein variants, has shed light on functional domains and mechanisms involved in flavivirus attachment and entry (for a review, see reference 33). An investigation by one of us on genotypic changes associated with host cell adaptation of the encephalitic flavivirus Murray Valley encephalitis virus (MVE) suggested an important role for residue 390 in the E protein in cell tropism and virulence (25). Asp_{390} found in the prototype virus was altered to His, Gly, Ala, or Asn after passage of MVE in a human adenocarcinoma (SW13) cell line, resulting in improved growth in the human cell line as well as virulence attenuation in mice. Residue 390 in the E protein of MVE is part of an Arg-Gly-Asp (RGD) sequence, the integrin-binding motif important in cell-extracellular matrix and cell-cell adhesion (42). This evidence prompted the first proposition for the location of the flavivirus receptor-binding site in a conserved, hydrophilic domain encompassing residue 390, with a possible role for integrins in the attachment of some flaviviruses (25). However, the RGD motif is not found in the E protein of all flaviviruses: it is found in Japanese encephalitis virus (JEV) (31), yellow fever virus (YFV) strain 17D (39), and the related RGE/T sequences in other members of the JEV serocomplex (5, 8, 47), but the corresponding amino acids in the E protein of the dengue viruses are unrelated (12, 26, 30) and deleted in TBE (29). Intriguingly, the RGD sequence in the vaccine

(17D) strain of YFV (39) arose as a consequence of host cell adaptation of the virulent Asibi strain, which has the corresponding amino acids Thr-Gly-Asp (11). Based on these sequence comparisons, it is unlikely that integrins are a general receptor for flavivirus attachment, in contrast to foot-and-mouth disease virus (16, 34) and coxsackievirus (40), which display a strict dependence on RGD-mediated integrin binding for host cell entry.

The crystal structure of the TBE E protein strongly supports a function in receptor binding of the hydrophilic region which harbors the RGD motif of some flaviviruses. This sequence is found in a solvent-exposed (FG) loop located in the immunoglobulin-like domain III of the E protein, and mutations which affect host cell tropism and virulence in different flaviviruses map in this region (37). In the current study, we introduced substitutions at the RGD motif in MVE with the use of an infectious clone. The phenotypic effects of changes in the putative flavivirus receptor-binding domain on virus growth, attachment, and entry in cultured cells and virulence in mice were examined.

MATERIALS AND METHODS

Viruses and cells. The MVE prototype strain MVE-1-51 (9) has been passaged 15 times in suckling mouse brain; a culture supernatant from C6/36 cells was used as working stock.

Vero (African Green monkey kidney), BHK-21 (baby hamster kidney), and SW13 (human adenocarcinoma) cells were all from the American Type Culture Collection (Bethesda, Md.) and maintained in Eagle's minimal essential medium (EMEM) plus nonessential amino acids and 5% fetal calf serum (FCS). C6/36 (*Aedes albopictus*) cells were grown in EMEM plus nonessential amino acids and 7% FCS at 28°C.

Plasmids. DNA fragments comprising the 5′ or 3′ half of the genome of MVE-1-51 were obtained by reverse transcription (RT)-PCR using expand reverse transcriptase and the Expand high-fidelity PCR system (both from Roche Diagnostics, Castle Hill, NSW, Australia). Oligonucleotide primers used in RT-PCR were designed to incorporate the promoter sequence for *T7* RNA polymerase plus an *Apa*I restriction endonuclease recognition site (underlined) at the 5′ terminus (5′-*GCTTGGGCCCTAATACGACTCACTATA*AGACGTTCATCT GCGTGAGCTTCCGATCTCAG-3′) and a *Not*I site (underlined) at the 3′ terminus (5′-*TATGCGGCCGC*AGATCCTGTGGTCTTCTCCCCCAT-3′) (nucleotides in italics are not present in the viral genome). Two additional internal primers corresponded to sequences encompassing a unique *Bam*HI site (underlined) in the middle of the genome (sense, 5′-GGAACTTCAGGATCCCCAA TAGTCAATAGC-3′; antisense, 5′-GCTATTGACTATTGGGGATCCTGAA GTTCC-3′). RT-PCR fragments 5,057 and 6,024 bp in size and corresponding to the 5′ and 3′ portions of the genome, respectively, were produced. Plasmids pM110, pM210, and pM310 were generated by ligation of independently produced 5′ 5,057-bp fragments, after digestion with *Apa*I and *Bam*HI, into plasmid pBR322* (2,793 bp) digested with the same enzymes and treated with shrimp alkaline phosphatase (Roche Diagnostics). This vector was derived from pBR322 by deletion of a 1,666-bp fragment encoding tetracycline resistance between the *Eco*RI and *Bsp*EI sites and insertion of the polylinker from pBluescript KS+ (Stratagene, La Jolla, Calif.) at the site of deletion. Plasmids pM116, pM211, pM212, pM213, and pM215 contain the full-length MVE cDNA. They were generated by ligation of independently produced 3′ 6,024-bp fragments cut with *Bam*HI and *Not*I into pM110 or pM210 digested with the same enzymes. Plasmids pM312′ and pM312″ were produced by replacement of the MVE 5′ terminus of clone pM212 with a 1,971-bp *Apa*I-*Xba*I fragment from pM310 or the adjacent sequence of 3,073 bp with an *Xba*I-*Bam*HI fragment from pM310, respectively.

Introduction of mutations at codon 390 in the E protein gene. A shuttle vector, pM212(X/B), was made by cloning a 3,073-bp *Xba*I-*Bam*HI fragment from pM212 into pBluescript II KS+ and subsequent deletion of the polylinker region between *Apa*I and *Bam*HI by digestion with the two restriction endonucleases, treatment with T4 DNA polymerase to create blunt ends, and religation. To produce a Gly_{390} mutant, a 563-bp *Pst*I-*Sac*I fragment from pM212(X/B) was exchanged with that obtained from RT-PCR amplification of nucleotides 1,593 to 5030 in the genome of MVE-1-51 passage variant P4/10 (25). The mutation was subcloned into pM212 by exchange of a 3,073-bp *Xba*I-*Bam*HI fragment with that containing the mutated E protein 390 codon.

A random site-directed mutagenesis approach for generating E protein 390 variants was employed with the use of the degenerate mutagenesis oligonucleotide 5′-GATTGATCTGCTTC/ANNTCCGCGGCCTACCACAAT-3′, which is complementary to a sequence in the MVE E gene from nucleotides 2121 to 2154 and contains the sequence for a *Sac*II site (underlined). A 563-bp *Pst*I-*Sac*I fragment (nucleotides 1950 to 2513 in the MVE genome) from pM212 was cloned into M13mp19 phage replicative form (RF) DNA for preparation of uridinylated single-stranded DNA from recombinant phage particles after infection of *Escherichia coli* strain CJ236. Mutagenesis was done as described (45); briefly, uridinylated single-stranded DNA (0.5 μg) was annealed with phosphorylated oligonucleotide (1 pmol) and converted into RF DNA using Sequenase (5 U; USB Corp., Cleveland, Ohio) and T4 DNA ligase (2 U; Pharmacia Biotech, Uppsala, Sweden). Plaques obtained following transfection of *E. coli* strain TG1 with the mutagenesis mix were screened by restriction enzyme digestion of RF DNA and tested for the presence of a *Sac*II site. The DNA was then subjected to sequence analysis using the Big-Dye terminator cycle-sequencing kit (PE Applied Biosystems, Foster City, Calif.) to detect mutations at codon 390. Mutations which gave rise to amino acid changes were cloned as *Pst*I-*Sac*I fragments from RF DNA samples into the transfer vector pM212(X/B) digested with the same enzymes prior to transfer into full-length clone pM212 as described above.

Transcription of RNA from full-length MVE cDNA clones. Plasmids containing the full-length MVE cDNA were digested with *Not*I and treated with Klenow fragment (Pharmacia Biotech) to create blunt ends. After extraction with phenol-chloroform and ethanol precipitation, linearized DNA was added to a transcription mix containing 0.5 U of T7 RNA polymerase (Promega, Madison, Wis.) and 1 U of RNase inhibitor (RNAGuard; Pharmacia Biotech, Uppsala, Sweden) per μl, 40 mM Tris-HCl (pH 7.9), 6 mM $MgCl_2$, 2 mM spermidine, 10 mM NaCl, 10 mM dithiothreitol, 1 mg of bovine serum albumin (BSA) per ml, 1 mM CAP analogue mG(5′)ppp(5′)G (Pharmacia Biotech), and 1 mM each ATP, UTP, and CTP. The mixture was incubated at 37°C for 5 min, GTP was added to 1 mM, and the incubation was continued at 37°C for 1 h. RNA transcripts were used directly in transfection experiments.

Transfection of BHK-21 and C6/36 cells. Transfection of BHK-21 cells was done by electroporation. Subconfluent cell monolayers were harvested with trypsin, washed twice in serum-free EMEM, and suspended in EMEM at 1.2×10^7 cells/ml. The cells (10^7) were mixed with in vitro-synthesized RNA in an electroporation chamber (0.4-cm gap; Life Technologies, Rockville, Md.) and subjected to two consecutive pulses at 250 V, 800 μF, and "low-ohm" setting using the Cell-Porator electroporation system I (Life Technologies). Cells were left at room temperature for 5 min, suspended in 24 ml of EMEM–5% FCS, and transferred to culture dishes for incubation at 37°C. Culture fluids were harvested after 3 days for plaque isolation and titration. For RNA transfection of C6/36 cells, lipofectin (6 μl; Life Technologies) was mixed with 0.4 ml of phosphate-buffered saline (PBS) and held at room temperature for 15 min, and then RNA transcript (0.2 μg) was added, and the mixture was applied to cells in a 35-mm dish (washed twice with PBS). After incubation at room temperature for 20 min, the transfection mix was removed, monolayers were washed once with PBS, and EMEM–7% FCS was added.

Virulence assays. Virulence assays were performed in 3-week-old Swiss White outbred mice as described (32). Virus stocks used in virulence assays were obtained by plaque purification on Vero cells followed by two rounds of amplification in C6/36 cells. Virus samples were serially diluted in Hanks' balanced salt solution (HBSS) containing 20 mM HEPES (pH 8.0) plus 0.2% BSA (HBSS-BSA), and 30 μl was inoculated into each animal by the intracranial (i.c.) or intraperitoneal (i.p.) route.

Infectivity assays. Vero cells (2×10^5/well) and SW13 cells (10^5/well) in 24-well Linbro dishes (ICN Biomedicals, Aurora, Ohio) were infected at ~0.1 PFU/cell, the virus was left to adsorb for 1 h at 37°C, and monolayers were washed twice with PBS before EMEM–5% FCS (1 ml) was added. At 16, 20, 24, and 28 postinfection (hpi), the culture supernatant was collected and stored at −70°C following the addition of HEPES buffer (pH 8.0) to 10 mM. Monolayers were washed once with PBS, and fresh medium (1 ml) was added. Virus growth samples from Vero and SW13 cells were titrated by plaque formation on Vero or SW13 cell monolayers, respectively, using six-well Linbro trays (ICN Biomedicals). Overlay medium for plaque assay contained EMEM plus 1% agar (Difco Laboratories, Irvine, Calif.) and 2% FCS in both cases. Plaques on Vero cells were visualized by adding neutral red stain (ICN Biomedicals; 0.02% [wt/vol] in 1% agar solution) at 4 to 5 days postinfection (dpi). Plaques on SW13 cells were visualized at 5 dpi after removal of agar overlay and staining with crystal violet (0.1% in 20% ethanol–H_2O).

For virus growth assays in C6/36 cells, monolayers (2×10^5 cells/well) in 24-well trays were infected with 0.1 C6/36 focus-forming unit/ml. After 1 h of adsorption, the monolayers were washed and 1 ml of EMEM–7% FCS was added. The cells were incubated at 28°C. Virus growth samples were collected between 20 and 42 hpi as above. Virus titration was performed by an immunofluorescence focus assay on C6/36 cell monolayers in 24-well dishes. Overlay medium contained EMEM–5% FCS–1% carboxymethyl cellulose (high viscosity; ICN Biomedicals; prepared as a 3% stock solution in water and autoclaved). At 3 dpi, monolayers were washed with PBS and fixed in ice-cold acetone-methanol (1:1). Foci of infection were detected using an anti-MVE hyperimmune ascitic fluid, fluorescein isothiocyanate-conjugated anti-mouse immunoglobulin G (IgG), (Silenus Laboratories, Hawthorn, Australia) and immunofluorescence microscopy.

Virus attachment and entry assays. For uptake assays, SW13 cell monolayers (60% confluent) in six-well trays were used after replacing the medium with HBSS-BSA. Virus samples (200 SW13 PFU in HBSS-BSA) were added to each well at room temperature. At specified times after virus addition, monolayers were washed three times with acid EMEM (pH 4.0, buffered with 20 mM

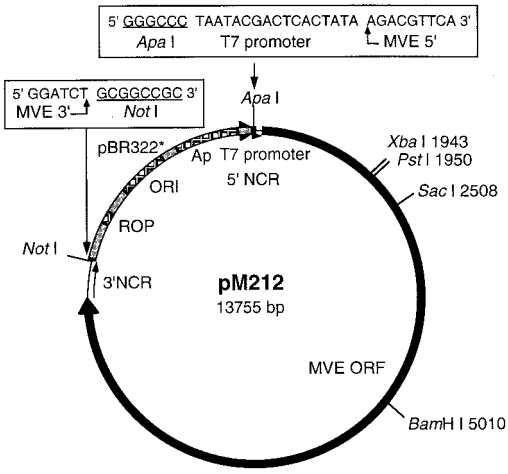

FIG. 1. Full-length infectious cDNA clone of MVE-1-51. Plasmid pM212 contains the full-length cDNA of MVE-1-51 (11,013 nucleotides), which includes an open reading frame (ORF) encoding a polyprotein of 3,434 amino acids (solid line). Restriction sites used in subcloning and genetic manipulations are shown (numbering is from the 5′-terminal nucleotide in MVE-1-51). Sequences at the 5′ (plus an *Apa*I site and T7 promoter sequence) and 3′ (plus a *Not*I site) termini of the viral genome are shown (boxed). The vector pBR322* is a deleted version of pBR322 (see Materials and Methods). The ampicillin resistance gene (Ap), the ROP gene, and the origin of DNA replication (ORI) are shown. NCR, noncoding region.

[2-*N*-morpholino]ethane-sulfonic acid; ICN Biomedicals). The monolayers were incubated with acid medium for 2 min, and the medium was aspirated and replaced with HBSS-BSA. The acid treatment inactivates bound and unbound virus but not virus which has undergone uptake by endocytosis (10, 18). Overlay agar was then added, and cells were incubated for 5 days to allow plaque development. A control monolayer for each virus sample was used for plaque titration in the absence of the acid treatment.

To confirm that bound but noneclipsed virus was completely inactivated by the acid treatment, SW13 cell monolayers (60% confluent) in six-well Libro trays were cooled to 4°C for 30 min after replacing medium with HBSS-BSA. Virus samples (400 SW13 PFU in HBSS-BSA) were added to each well, and incubation was continued at 4°C for 60 min. Unbound virus was removed by two washes of the monolayers with HBSS-BSA, and acid treatment was performed as above. The monolayers were left under HBSS-BSA for a further 10 min at 37°C prior to the addition of an agar overlay (see above) and incubated for 5 days at 37°C to allow plaque development. For each virus sample, a control monolayer which was not subjected to acid treatment was included.

Heparin inhibition of virus attachment. The effect of heparin on MVE infection of Vero, SW13, and BHK-21 cells was assayed by preincubation of virus samples (100 to 200 PFU in 100 μl of HBSS-BSA) with heparin (20 to 200 μg/ml; Sigma, St. Louis, Mo.) for 15 min prior to addition to cell monolayers (incubated with 200 μl of HBSS-BSA containing 20 to 200 μg of heparin per ml). After 1 h, agar overlay medium (see above) was added to allow plaque development.

The effect of heparin on virus attachment was assayed in Vero and SW13 cells by preincubation of virus samples (400 PFU in 100 μl of HBSS-BSA) at 4°C with heparin (20 to 200 μg/ml) prior to addition to chilled (4°C, 30 min) cell monolayers (incubated with 200 μl of HBSS-BSA containing 20 to 200 μg of heparin per ml) followed by incubation on ice for 1 h. Unbound virus was removed by two washes of the cell monolayers with HBSS-BSA, and the monolayers were held at 37°C for 10 min before addition of an agar overlay.

RESULTS

Full-length infectious cDNA clones of MVE-1-51. cDNA fragments corresponding to the 5′ and 3′ halves of the MVE genome and overlapping at a unique *Bam*HI site at nucleotide 5010 were generated by RT-PCR. A 5′ *Apa*I restriction site, a T7 RNA promoter sequence, and a 3′ *Not*I site were incorporated into the PCR primers to allow cloning of PCR fragments into a low-copy-number plasmid (pBR322*) and in vitro synthesis of full-length RNA transcript. These transcripts contain an authentic 5′ end but six additional nucleotides (*Not*I site) at the 3′ end (Fig. 1). Five full-length MVE cDNA clones (pM116, pM211, pM212, pM213, and pM215) comprising two of the three independently derived 5′ halves and five independently derived 3′ halves of the genome were generated. Two additional clones were produced from the third 5′ half of the MVE genome by replacement of the MVE 5′ end of clone pM212 with a 1,971-bp *Apa*I-*Xba*I fragment (pM312′) or the adjacent sequence of 3,073 bp with an *Xba*I-*Bam*HI fragment (pM312″). All plasmids encoding the full-length MVE cDNA were stably propagated in *E. coli* MC1061.1 cells but required incubation for 30 h at 37°C for sufficient yield.

TABLE 1. Infectivity of MVE full-length cDNA clone-derived RNAs in mammalian and insect cells

MVE full-length clone	Infectivity	
	C6/36 cells[a] (infectious centers/μg of RNA)	BHK-21 cells[b] (PFU/ml)
pM116	<10	4.6×10^3
pM211	<10	<100
pM212	200	1.4×10^4
pM213	30	6.5×10^3
pM215	100	ND
pM312′	30	<100
pM312″	<10	ND

[a] Infectious centers on C6/36 cell monolayers were detected by immunofluorescence microscopy at 3 days after transfection.

[b] Progeny virus in the culture fluid from BHK-21 cells at 72 h after transfection was counted by plaque formation on Vero cells. ND, not determined.

In vitro-synthesized RNA transcripts were first tested for infectivity in mosquito (C6/36) cells using a Lipofectin-based transfection protocol (~0.5 μg RNA/10^6 cells). RNA transcripts from four clones (pM212, pM213, pM215, and pM312′) gave rise to progeny virus and MVE-specific immunofluorescence foci in the monolayers at 3 days posttransfection (Table 1). RNA transcript derived from five of the seven full-length cDNA clones were also tested for infectivity in vertebrate (BHK-21) cells transfected by electroporation (~1 μg of RNA/10^7 cells). Progeny virus was recovered for transcripts from three clones (pM116, pM212, and pM213; Table 1). Infectivity of the different RNA transcripts in C6/36 cells did not fully correspond to that in BHK-21 cells (e.g., clones pM116 and pM312′). This was not investigated further but was probably due to the low infectivity of the transcripts, resulting in variable success in the productive transfection of cells. Plasmid pM212, which gave rise to the highest infectious titers in both BHK-21 and C6/36 cells in the initial screening procedure, was selected for use in the subsequent experiments. The transfection efficiency of RNA derived from this clone was ~100 infectious centers/μg of RNA in both cell lines tested. This value was more than 1,000-fold lower than that observed in similar transfections of C6/36 and BHK-21 cells using MVE virion RNA (~2×10^5 infectious centers/μg of RNA); it was also significantly lower than the infectivity of RNA derived from YFV (38) or TBE (28) cDNA clones but comparable to or greater than the transfection efficiencies of RNA transcripts from other flavivirus cDNA clones (17, 20, 23, 46). Since virus progeny produced in cells transfected with MVE cDNA clone pM212-derived RNA had growth and virulence properties similar to those of the parent virus (see below), it appears that replication results in the repair of a defect present in the in vitro-synthesized genomic RNA. This could involve removal of some of the additional nucleotides at the 3′ end of infectious clone-derived RNA.

MVE mutants with substitutions at residue 390 in the E protein. Asp_{390} in the MVE E protein is part of an RGD motif in the

TABLE 2. Mutations at codon 390 in the E protein and biological properties of mutants

Amino acid	Codon[a]	Plaque size in Vero cells[b]	Growth phenotype[c]			Heparin inhibition in SW13 cells[d]	Virulence[e]
			Vero cells	SW13 cells	C6/36 cells		
Asp_{390}	GAU + *Sac*II	Large	+++	+	++	+	Virulent
Glu_{390}	GAG + *Sac*II	Large	+++	+	ND	+	Virulent
Gly_{390}	GGC	Small	+	+++	+	+++	Attenuated
Ala_{390}	GCG + *Sac*II	Intermediate	++	++	ND	+++	ND
Val_{390}	GUG + *Sac*II	Intermediate	++	++	++	++	ND
Leu_{390}	CUG + *Sac*II	Intermediate	++	+	ND	++	ND
Thr_{390}	ACG + *Sac*II	Large	++	+	ND	+	Virulent
Tyr_{390}	UAU + *Sac*II	Large	++	+	++	+	Intermediate
Gln_{390}	CAG + *Sac*II	Large	++	++	++	+	Virulent
His_{390}	CAU + *Sac*II	Small	+	+++	+	+++	Attenuated
Lys_{390}	AAG + *Sac*II	Large	++	+	ND	+	ND

[a] Codons for residue 390 in E protein mutants are shown with the nucleotides that differ from those in the sequence of MVE-1-51 E (GAC) underlined. The presence of additional nucleotide mutations giving rise to a *Sac*II site (CCGCGG) is indicated.
[b] Plaque size (diameter) in Vero cells at 4 dpi (monolayers stained 3 dpi) is shown. Large, 1.5 to 2.0 mm; intermediate, ~1 mm; small, ≤0.5 mm.
[c] Derived from Fig. 2. +, poor growth; ++, intermediate growth; +++, efficient growth. ND, not determined.
[d] Derived from Fig. 4. +, low inhibition; ++, intermediate inhibition; +++, high inhibition.
[e] Derived from Fig. 5.

putative flavivirus receptor-binding domain. It is subject to replacement with other amino acids as a result of host cell adaptation of MVE and is also a determinant for virulence in mice (25). To investigate the impact of single amino acid changes at this site on cell tropism, virus entry, and virulence in the context of an otherwise identical genetic background, the codon for Asp_{390} in MVE full-length clone pM212 was mutated to that for one of 10 other amino acids. A random mutagenesis approach was used which relied on a degenerate oligonucleotide to introduce randomized codons at residue 390 as well as silent substitutions generating a unique *Sac*II site. A Gly_{390} mutant was produced by substituting a cDNA fragment encompassing codon 390 in pM212 with that obtained by RT-PCR amplification from a variant virus (P4/10) which had been selected by passage in SW13 cells (25). The collection of E protein 390 mutants obtained is shown in Table 2. It includes the conservative replacement of Asp_{390} with Glu and the nonconservative substitutions with small aliphatic residues (Gly or Ala), aliphatic hydrophobic residues (Val or Leu), an aliphatic polar residue (Thr), an aromatic polar residue (Tyr), an acidic amide (Gln), a polar weakly basic residue (His), and a basic residue (Lys). A clone unchanged at Asp_{390} but with silent mutations introducing the *Sac*II site was also generated.

RNA was transcribed from each of the 11 mutated full-length clones and transfected into BHK-21 cells. Culture fluids were collected after 3 days and tested for the presence of infectious virus by plaque titration on Vero cells. Each of the E protein 390 mutants gave rise to viable progeny virus; however, their plaque morphology differed markedly (Table 2). In particular, the His_{390} and Gly_{390} viruses produced very small plaques. Mutant virus stocks were obtained after amplification of single plaques once each in C6/36 and Vero cells, with the exception of the His_{390} and Gly_{390} viruses, which were amplified twice in C6/36 cells to obtain stocks of sufficiently high titers. The sequences from nucleotides 960 to 2500 encompassing the entire E protein gene were confirmed for each of the mutants by direct sequencing on RT-PCR fragments obtained from intracellular RNA extracted from cells used for virus amplification.

Growth of E protein 390 mutants in vertebrate and invertebrate cells. A previous investigation demonstrated that the substitution of Asp_{390} with His in the E protein of MVE resulted in altered virus growth in Vero and SW13 cells (25). Although the nucleotide sequences of the E protein genes of the passage variant and prototype virus were otherwise identical, the presence of differences elsewhere in the genome could not be excluded. To confirm that residue 390 is part of an E protein domain that functions as a determinant of host cell tropism and to extend this study to a wide range of amino acid substitutions at residue 390, ten 390 mutants with otherwise identical genetic backgrounds were examined for growth in Vero, SW13, and C6/36 cells. Infections were performed at 0.1 PFU/cell in one-step growth experiments. Virus titers of growth samples were determined on the corresponding cell lines by plaque (Vero and SW13) or immunofluorescence focus assays and (C6/36).

Growth in Vero cells of infectious clone (pM212)-derived virus vM212 and the control Asp_{390} mutant virus was compared with that of prototype virus MVE-1-51. At each time point between 16 and 28 hpi, similar extracellular virus titers were detected in the single-step growth curves for these viruses (Fig. 2).

Growth of the E protein 390 mutants was tested in two separate experiments in both Vero and SW13 cells with repeat determinations of growth phenotypes of Gly_{390} and His_{390} viruses shown for comparison (Fig. 2). In Vero cells all E protein 390 mutants showed lower titers between 16 and 28 hpi than the Asp_{390} virus. Two of the mutants (Gly_{390} and His_{390}) produced titers more than 100-fold below those of the Asp_{390} virus. The other six mutants had intermediate growth properties, with titers often reduced 10-fold. The conservative Asp_{390}-to-Glu mutation gave growth properties most similar to those of the Asp_{390} virus, reaching identical titers at 28 hpi. There was a strict correlation between plaque size of the mutants on Vero cell monolayers and growth phenotypes (Table 2). In the two growth assays shown, the monolayers were fixed at 24 hpi for detection of the number of virus-infected cells by immunofluorescence assay. There was little or no difference in the percentage of MVE-infected cells between any of the mutants tested (data not shown).

Most of the changes at residue 390 in the E protein resulted in (up to 100-fold) improved growth in SW13 cells compared to the Asp_{390} virus (Fig. 2). Highest titers were observed for the Gly_{390} and His_{390} mutants, the two viruses that grew most poorly in Vero cells. There was little or no difference in the number of infected cells between all viruses tested, as deter-

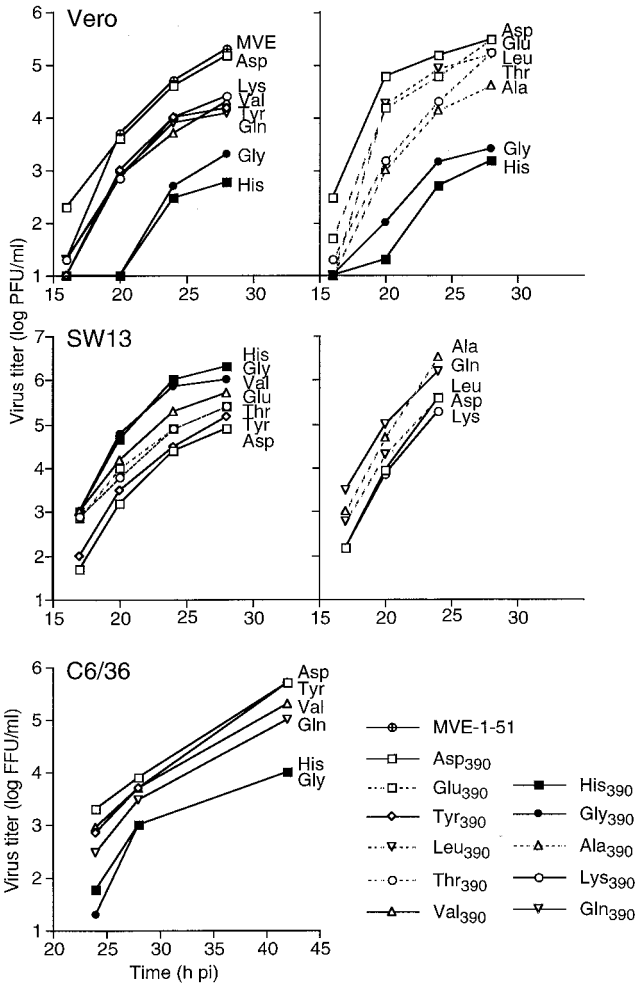

FIG. 2. Growth of E protein 390 mutants in cell culture. Vero, SW13, and C6/36 cells were infected with MVE-1-51, the Asp_{390} control virus, or 1 of 10 E protein 390 mutants at multiplicity of ~0.1, determined for each cell type. Unbound virus was removed after 1 h of adsorption, and growth medium was added. At 16, 20, 24, and 28 hpi, supernatants were collected from Vero and SW13 cells for titration of virus infectivity, in the respective cell types. For growth assays in C6/36 cells, supernatant samples were taken at 24, 28, and 44 hpi, and virus titers were determined as focus-forming units (FFU) by immunofluorescence in C6/36 cells. Results for Vero and SW13 growth assays are from two separate experiments (shown in different graphs).

mined by immunofluorescence staining for MVE antigen at 24 hpi (data not shown).

The single-step growth curves of infectious clone-derived viruses vM212 and Asp_{390} in C6/36 cells were indistinguishable from that of prototype virus MVE-1-51 (data not shown). Subsequently, the growth properties of five E protein 390 mutants were compared to that of the Asp_{390} virus in the mosquito cell line (Fig. 2). There was no detectable virus release at 20 hpi. At later time points, titer of two mutants, Gly_{390} and His_{390}, were 20- to 100-fold lower than those for the Asp_{390} control virus. The Gln_{390} virus showed intermediate growth, and titers for the Val_{390} and Thr_{390} mutants were only slightly lower than titers for the Asp_{390} control. Accordingly, the effect of different amino acid changes at residue 390 in the E protein on virus growth in Vero and C6/36 cells showed a similar pattern.

Effect of residue 390 in the E protein on entry kinetics into SW13 cells. The entry kinetics into SW13 cells of the His_{390} mutant, which showed improved growth in this cell line, was

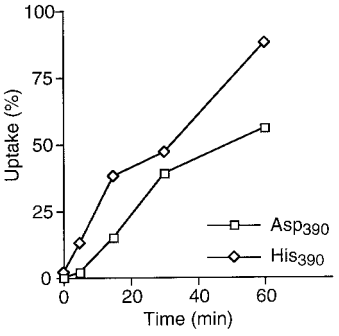

FIG. 3. Uptake of MVE into SW13 cells. The kinetics of uptake of the Asp_{390} control and His_{390} mutant viruses into SW13 cells was determined as described in Materials and Methods. Percent uptake for each time point is expressed as the ratio of the number of plaques obtained after acid treatment and the number of plaques obtained on a control monolayer in the absence of acid treatment.

compared to that of the Asp_{390} control virus. Following incubation of virus on cell monolayers at room temperature for 5, 15, 30, and 60 min, unbound virus was removed and bound but noneclipsed virus was inactivated by the addition of acidic (pH 4.0) medium. Agar overlay medium was added, and plaques were allowed to develop over 5 days. The acid wash induces an irreversible conformational change in the E protein (1) which inactivates virus infectivity (10, 18). This was corroborated in control experiments, in which plaque formation was completely inhibited when adsorption was performed at 4°C for 1 h prior to the addition of acid medium. The kinetics of virus entry of the His_{390} mutant was significantly faster than that of the Asp_{390} virus, with greater than twofold differences seen at all time points (Fig. 3). Similar results were obtained in two repeat experiments. These data suggest that amino acid substitutions at residue 390 can result in more efficient virus uptake into SW13 cells. Consequences of enhanced uptake kinetics would be (i) a faster growth kinetics and (ii) an increase in the relative infectivity in the cell line used to generate the single-step growth curves. Collectively, these factors are likely to account for the improved growth phenotypes of most E protein 390 mutants observed in SW13 cells.

Differential inhibition of virus infectivity by heparin is determined by amino acids at residue 390 in the E protein. The improved entry kinetics into SW13 cells of one of the E protein 390 mutants relative to the control virus, the selection of amino acid changes at residue 390 during host cell adaptation of MVE (25), and the location of residue 390 in a domain with putative receptor-binding function (25, 37) suggest a critical role for this site in virus attachment to host cell receptors. Given that host cell adaptation of some other viruses correlated with an increased dependence on GAGs in virus attachment (3, 21, 43) and that a role for GAGs in dengue-2 virus attachment to vertebrate cells has been documented (7), we tested the effect of heparin on infection of Vero, SW13, and BHK cells with prototype MVE and E protein 390 mutant viruses.

Heparin had little effect on the infectivity of MVE-1-51 in Vero and SW13 cells. Preincubation of a virus inoculum (~200 PFU) with heparin at high concentrations (200 to 400 μg/ml) reduced plaque numbers by <20% in Vero and ~25% in SW13 cells (data not shown). The control Asp_{390} virus and the Gly_{390}, His_{390}, and Lys_{390} mutants were similarly tested using heparin concentrations from 50 to 200 μg/ml (Fig. 4A). The Asp_{390} virus showed <5% reduction in plaque numbers in Vero cells at all heparin concentrations tested, up to 28% reduction in plaque numbers in SW13

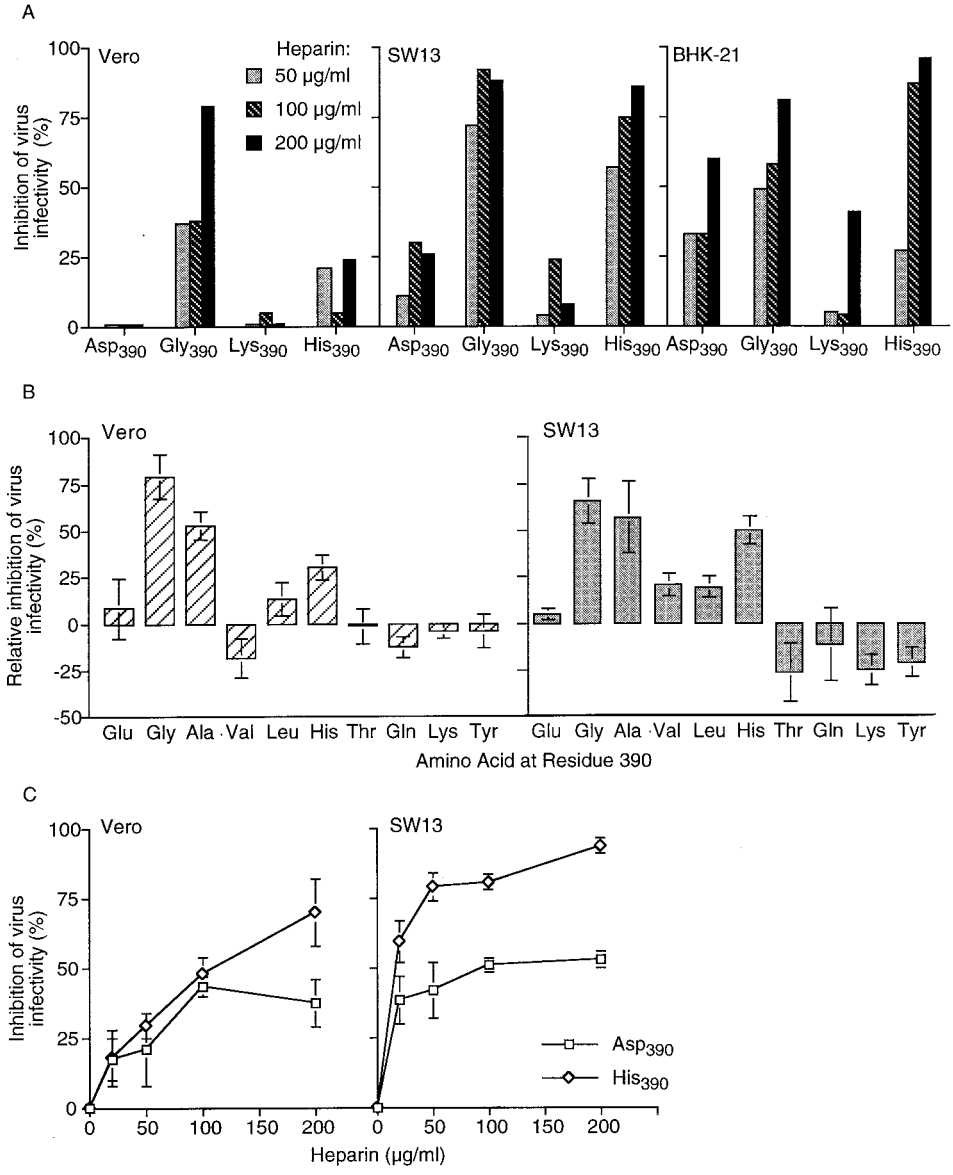

FIG. 4. Inhibition by heparin of virus infectivity in Vero, SW13, and BHK cells. (A) The Asp_{390} control and His_{390}, Gly_{390}, and Lys_{390} mutant viruses (200 PFU) were incubated with heparin (0, 50, 100, and 200 μg/ml) prior to their addition to cells pretreated with HBSS-BSA containing heparin at 0, 50, 100, or 200 μg/ml. Agar overlay was added to allow plaque formation after 1 h of adsorption at 37°C. Inhibition by heparin was calculated using the formula [(plaque number on nontreated cells − plaque number on heparin-treated cells)/(plaque number from non-treated cells)] × 100. (B) Inhibition of infectivity by heparin (200 μg/ml) of 10 E protein 390 mutants was assayed in parallel with the Asp_{390} control virus as in panel A. The percent inhibition by heparin of the Asp_{390} virus is subtracted from that for the E protein 390 mutants obtained in the same experiment. Results (mean and standard error) from three independent experiments are shown for each mutant. (C) Inhibition by heparin of virus binding to Vero and SW13 cells. The Asp_{390} control virus and the His_{390} mutant were incubated with heparin (0, 20, 50, 100, or 200 μg/ml) for 15 min at 4°C and then added to chilled Vero or SW13 cells treated with heparin (0 to 200 μg/ml). After 1 h of adsorption at 4°C, cell monolayers were washed, and agar overlay was added to allow plaque development. Percent inhibition by heparin is calculated as in panel A. Results (mean and standard error) from two independent experiments are shown.

cells, and 30 to 60% plaque reduction in BHK-21 cells. In contrast, the Gly_{390} mutant showed a much greater sensitivity to heparin inhibition. Plaque numbers in Vero cells were reduced by up to 80%, in SW13 cells by 70 to 88%, and in BHK-21 cells by 50 to 80% depending on the dose of heparin used. The His_{390} mutant showed 5 to 20% reduction in plaque numbers in Vero cells at 50 to 200 μg of heparin per ml and a greater reduction in SW13 cells (60 to 80%) and BHK-21 cells (28 to 95%). The infectivity of the Lys_{390} mutant was as or less susceptible to inhibition by heparin as the Asp_{390} control virus (5% in Vero, 5 to 20% in SW13, and 10 to 40% in BHK-21 cells).

The effect of heparin on infectivity was then tested for each of the 10 E protein 390 mutants in comparison to the control Asp_{390} virus using 200 μg of heparin per ml (Fig. 4B). Positive values indicate reduction in plaque numbers above and negative values indicate reduction below that with the Asp_{390} control virus. In addition to the Gly_{390} and His_{390} mutants, infectivity of the Ala_{390} mutant in Vero and SW13 cells was also inhibited significantly more by heparin than that of the Asp_{390} virus (Fig. 4B). The other mutants tested were not significantly different from the Asp_{390} virus (Glu_{390} and Gln_{390}) or were somewhat less sensitive to heparin inhibition in SW13 cells

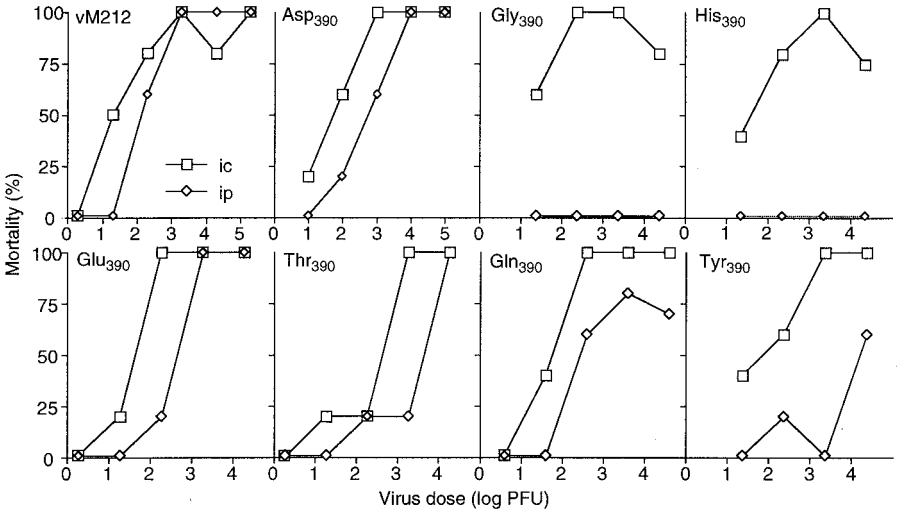

FIG. 5. Virulence of infectious clone-derived MVE and E protein 390 mutants. Virus stocks were diluted 10-fold serially in HBSS-BSA and used to inoculate 21-day-old Swiss outbred mice in groups of five by the i.p. or i.c. route. Mortality was recorded for 14 days.

(Thr_{390}, Lys_{390}, and Tyr_{390}). The susceptibility to heparin inhibition of SW13 cell infectivity of the Val_{390} and Leu_{390} viruses was marginally greater (~20%) than that of the Asp_{390} virus (reproduced in three experiments).

Heparin inhibits entry of MVE into Vero and SW13 cells. To confirm that heparin inhibits virus binding or entry into cells, an entry assay was performed (Fig. 4C). Ice-cold mixtures of virus (Asp_{390} control or His_{390} mutant virus) and heparin (20 to 200 μg/ml) were added to chilled Vero or SW13 cell monolayers and held for 1 h at 4°C for binding to occur without uptake by endocytosis. We found that the effect of heparin on virus infectivity was markedly increased when virus adsorption was performed at 4°C and the heparin-treated virus inoculum was completely removed prior to the addition of an agar overlay (compare Fig. 4A and C). The infectivity of the His_{390} mutant was inhibited by more than 50% at 20 and 200 μg of heparin per ml in SW13 and Vero cells, respectively. In contrast, the inhibition by heparin of entry of the Asp_{390} control virus resulted in a plateau of not greater than 50% reduction of infectivity in both cell lines, suggesting that the Asp_{390} virus can enter these cell lines by a mechanism which does not involve virus binding to cell surface GAGs. It is notable that Vero cells were significantly less susceptible than SW13 cells to inhibition by heparin in both binding and infectivity assays (Fig. 4A and C), suggesting a greater dependence on GAGs of MVE entry into SW13 than Vero cells.

Virulence of E protein 390 mutants. Mouse virulence of full-length MVE clone (pM212)-derived virus vM212 was determined by inoculating 3-week-old Swiss outbred mice with 10-fold serial dilutions of plaque-purified virus stock i.c. or i.p. (24, 32). Comparison of i.c. versus i.p. 50% lethal dose (LD_{50}) values, which did not differ by more than 10-fold, showed that vM212 was virulent (Fig. 5). The Asp_{390} virus which was used as a control for the other infectious clone-derived variants was also virulent by this criterion. Of the six E protein 390 mutants tested for mouse virulence, the Glu_{390}, Gln_{390}, and Thr_{390} mutants were also considered virulent. The Gly_{390} and His_{390} mutants were attenuated, as they induced no mortality by i.p. inoculation despite having i.c. LD_{50} values (<50 PFU) similar to that of the Asp_{390} virus. The Tyr_{390} mutant showed an approximately 100-fold difference between the i.c. and i.p. LD_{50} values and is considered intermediate in virulence.

DISCUSSION

Functional role of the putative flavivirus receptor-binding domain in cell tropism and attachment/entry. We have examined the functional role of the putative flavivirus receptor-binding domain in virus entry, host cell tropism, and pathogenesis in mice. In the E protein of MVE, this domain contains the RGD integrin-binding motif. The codon for Asp_{390}, which is part of the RGD motif, was targeted by site-directed mutagenesis using a full-length cDNA clone. Infectious clone-derived control virus vM212 was indistinguishable from the prototype virus, MVE-1-51, in growth in Vero cells and virulence in mice. All E protein 390 mutants were viable and produced plaques in Vero, SW13, and BHK-21 cells; however, marked differences in growth properties were observed. Replacement of Asp_{390} with small aliphatic (Gly or Ala) or a weakly basic (His) amino acid resulted in the most significant changes in virus growth; a 50- to 100-fold reduction in growth in Vero and C6/36 cells and >10-fold enhancement of growth in SW13 cells was seen in comparison with an Asp_{390} control virus. The other mutants showed smaller differences, but growth in Vero cells was always less efficient than that of the Asp_{390} virus and comparable or improved in SW13 cells (Table 2). The observation that MVE is largely tolerant to a wide range of changes at the third amino acid of the RGD motif suggests that these changes do not alter the structure of the E protein such that replication in cultured cells is inherently impaired. This contrasts with the neighboring Gly_{389}, which, when replaced with Ala, destabilizes the structure of the E protein in YFV 17D (49). A Gly is found at the corresponding position in almost all flaviviruses, whereas Asp_{390} (MVE E protein sequence numbering) is not highly conserved. A comparison of the efficiencies of RNA synthesis of wild-type and E protein 390 variants has revealed no significant difference when identical numbers of cells were infected (A. Thompson and L. Dalgarno, personal communication).

Analysis of E protein 390 mutants confirmed the significance of this residue as a determinant of host cell tropism. Given that residue 390 is located in the putative receptor-binding domain (7, 37), the most likely functional consequence of substitutions at this position is an altered receptor interaction. Interestingly, the most pronounced changes in growth phenotypes were

found for three mutants which were described in an earlier study of MVE variants selected by serial passage in SW13 cells (25). However, most SW13-passaged variants had other changes in the E protein in addition to the substitution of Asp_{390}. In the present investigation the derivation of the Gly_{390}, His_{390}, and Ala_{390} mutants from an infectious clone ascertained an otherwise identical genetic background.

In this study we provide conclusive evidence that the putative flavivirus receptor-binding domain is a functional determinant for virus entry into cells. Previous work has given suggestive support for the involvement of this domain in attachment and entry. First, variants of MVE with altered host cell tropism and virulence properties had substitutions at residue 390 (25), located in a hydrophilic region corresponding to the FG loop in the E protein crystal structure of TBE (37). Second, neutralization escape mutants of TBE had amino acid replacements at residues 384 and 387, both spatially proximal to the FG loop, and were attenuated for virulence in mice (13, 14). Third, based on the structure of the TBE E protein, the FG loop is exposed on the virion surface and meets the physical requirements for receptor binding (37). Fourth, the E proteins of several flaviviruses (e.g., MVE, JEV, and YFV) contain within the FG loop an RGD integrin-binding motif, utilized by other viruses for attachment to host cells. Mutations leading to the loss or gain of this RGD motif were found following host cell adaptation by serial passaging of MVE (25) and YFV (11). Here we show that single amino acid changes in the FG loop of the E protein of MVE give rise to variants with altered attachment and entry phenotypes in comparison with the prototype virus. Two assays were used to analyze the early events of virus infection. An uptake assay, in which noneclipsed virus particles were inactivated by acid treatment, clearly demonstrated the faster entry kinetics of a His_{390} mutant relative to the control virus. The converse has been reported for Vero cells, in which the penetration of His_{390} and Ala_{390} variants was found to be significantly delayed relative to that of the parent virus, MVE-1-51 (23a). Given that the rate of virus uptake is most likely a consequence of the efficiency of interaction between the virus and a host cell receptor(s), the differential entry kinetics of the two viruses suggests that the E protein domain encompassing residue 390 functions in virus attachment. This is strongly supported by the result of the second attachment-entry assay, which showed a striking correlation between growth properties in cultured cells and susceptibility to heparin inhibition of virus infectivity, both of which were influenced by the amino acid at residue 390 in the E protein (Table 2). This is consistent with the interpretation that substitutions at residue 390 in the putative receptor-binding domain can alter receptor usage, as reflected in the differential involvement of cell surface GAGs in virus entry.

Role of GAGs in entry of an encephalitic flavivirus. Heparan sulfate on the cell surface plays a role in the attachment of a number of viruses (3, 21, 41, 43), including that of dengue-2 virus, to mammalian cells (7, 15). GAG-mediated virus attachment is inhibited by heparin, a highly sulfated form of heparan sulfate. We tested whether infectivity of MVE in Vero, SW13, and BHK-21 cells was sensitive to inhibition by heparin and found a dose- and cell type-dependent effect for the prototype virus. This inhibitory effect of heparin on virus infectivity was significantly greater for three of the 390 mutants (Gly_{390}, His_{390}, and Ala_{390}). Two mutants (Val_{390} and Leu_{390}) showed an intermediate phenotype of susceptibility to heparin, whereas the others did not differ markedly from the Asp_{390} virus (Table 2). The observation that substitutions at residue 390 in the E protein can render MVE infectivity highly susceptible to heparin inhibition strongly suggests that this site is in close proximity to a GAG-binding domain in the E protein and can directly influence the interaction between virus and cell surface GAGs. Support for this interpretation has been obtained in an investigation of JEV variants adapted to growth in SW13 cells which had single amino acid change located in a loop directly opposing residue 390 according to the crystal structure of the TBE E protein (unpublished data). Nevertheless, it cannot be excluded that substitutions at residue 390 in the MVE and JEV E proteins alter the overall conformation of the protein and influence a distantly located domain important for virus attachment and entry. The reason why small uncharged (Gly and Ala) or small polar (His) amino acids at residue 390 would enhance virus binding to GAGs is not immediately apparent. GAG-binding domains are characteristically rich in basic amino acids which are flanked by hydrophobic residues (41). An attractive hypothesis is that the positively charged Arg in the RGD motif or other basic residues in a region spatially proximal in the protein structure bind to negatively charged GAGs and that this interaction is subject to steric and charge hindrance depending on the amino acid at residue 390.

The altered attachment and entry properties of some of the MVE E protein 390 mutants have revealed a GAG-dependent entry mechanism that could be inhibited almost completely by heparin. However, the significance of cell surface GAGs for the entry of natural isolates of MVE, which are unaltered in the RGD motif (24), is unclear in view of the partial inhibition of infectivity by heparin found for the prototype virus. The latter observation is consistent with the view that one or more alternative cell surface molecules lacking heparan sulfate moieties can function as receptors for virus attachment. We have speculated that integrins are a candidate receptor for MVE and other flaviviruses that possess an RGD integrin-binding motif (25), but have been unable to demonstrate this interaction using RGD motif-containing peptides in attempts to inhibit the infectivity of MVE (E. Lee, unpublished data). A similar conclusion was reached by van der Most et al. (49), who tested a putative function of integrins as receptors for YFV 17D. From the present study, it is apparent that experiments attempting to block one specific virus-host cell receptor interaction must take into consideration the use of alternative (e.g., GAG dependent) mechanisms for attachment and entry which may gain in significance when the first pathway is blocked.

Effect of GAG dependence in virus entry on virulence. Residue 390 in the E protein of MVE is also a determinant of pathogenesis in mice. Of six mutants tested, two (Gly_{390} and His_{390}) had lost neuroinvasiveness and were considered fully attenuated by the criteria of the virulence assay. However, their growth in the brain following i.c. inoculation was not notably changed, based on the average time to death of the infected animals. The loss of neuroinvasiveness of the Gly_{390} and His_{390} mutants most likely reflects their inefficient replication in extraneural tissues. Thus, the correlation of altered cell tropisms and of increased susceptibility of virus entry to inhibition by heparin with the type of amino acid at residue 390 extends to virulence phenotypes in mice. A parallel may be drawn between the attenuated 390 mutants of MVE and Sindbis virus variants, which were derived from cell culture adaptation, attenuated, and dependent on GAG-mediated attachment for infectivity in cultured cells (3, 4, 21). It was argued that the loss of virulence of the Sindbis virus variants was a consequence of their high affinity for GAGs and that after peripheral inoculation these attenuated variants are concentrated and inactivated in the liver, an organ highly enriched in GAGs, thus limiting their ability to spread to the brain. A similar scenario has been proposed for the attenuation of foot-and-mouth disease virus (43) and may explain the loss of neuroinvasiveness of E

protein 390 mutants of MVE and other flavivirus variants attenuated by host cell adaptation.

ACKNOWLEDGMENTS

We are grateful to L. Dalgarno and R. C. Weir for the provision of unpublished sequence data for MVE-1-51.

REFERENCES

1. **Allison, S. L., K. Stiasny, K. Stadler, C. W. Mandl, and F. X. Heinz.** 1999. Mapping of functional elements in the stem-anchor region of tick-borne encephalitis virus envelope protein E. J. Virol. **73:**5605–5612.
2. **Bernfield, M., M. Götte, P. W. Park, O. Reizes, M. L. Fitzgerald, J. Lincecum, and M. Zako.** 1999. Functions of cell surface heparan sulfate proteoglycans. Annu. Rev. Biochem. **68:**729–777.
3. **Byrnes, A. P., and D. E. Griffin.** 1998. Binding of Sindbis virus to cell surface heparan sulfate. J. Virol. **72:**7349–7356.
4. **Byrnes, A. P., and D. E. Griffin.** 2000. Large-plaque mutants of Sindbis virus show reduced binding to heparan sulfate, heightened viremia, and slower clearance from the circulation. J. Virol. **74:**644–651.
5. **Castle, E., T. Nowak, U. Leidner, G. Wengler, and G. Wengler.** 1985. Sequence analysis of the viral core protein and the membrane-associated proteins V1 and NV2 of the flavivirus West Nile virus and of the genome sequence for these proteins. Virology **145:**227–236.
6. **Chambers, T. J., C. S. Hahn, R. Galler, and C. M. Rice.** 1990. Flavivirus genome organization, expression, and replication. Annu. Rev. Microbiol. **4:**649–688.
7. **Chen, Y., T. Maguire, R. E. Hileman, J. R. Fromm, J. D. Esko, R. J. Linhardt, and R. M. Marks.** 1997. Dengue virus infectivity depends on envelope protein binding to target cell heparan sulfate. Nat. Med. **3:**866–871.
8. **Coia, G., M. D. Parker, G. Speight, M. E. Byrne, and E. G. Westaway.** 1988. Nucleotide and complete amino acid sequences of Kunjin virus: definitive gene order and characteristics of the virus-specified proteins. J. Gen. Virol. **69:**1–21.
9. **French, E. L.** 1952. Murray Valley encephalitis: isolation and characterization of the aetiological agent. Med. J. Aust. **1:**100–103.
10. **Gollins, S. W., and J. S. Porterfield.** 1986. The uncoating and infectivity of the flavivirus West Nile on interaction with cells: effects of pH and ammonium chloride. J. Gen. Virol. **67:**1941–1950.
11. **Hahn, C. S., J. M. Dalrymple, J. H. Strauss, and C. M. Rice.** 1987. Comparison of the virulent Asibi strain of yellow fever virus with the 17D vaccine strain derived from it. Proc. Natl. Acad. Sci. USA **84:**2019–2023.
12. **Hahn, Y. S., R. Galler, T. Hunkapiller, J. M. Dalrymple, J. H. Strauss, and E. G. Strauss.** 1988. Nucleotide sequence of dengue 2 RNA and comparison of the encoded proteins with those of other flaviviruses. Virology **162:**167–180.
13. **Holzmann, H., F. X. Heinz, C. W. Mandl, F. Guirakhoo, and C. Kunz.** 1990. A single amino acid substitution in envelope protein E of tick-borne encephalitis virus leads to attenuation in the mouse model. J. Virol. **64:**5156–5159.
14. **Holzmann, H., K. Stiasny, M. Ecker, C. Kunz, and F. X. Heinz.** 1997. Characterization of monoclonal antibody-escape mutants of tick-borne encephalitis virus with reduced neuroinvasiveness in mice. J. Gen. Virol. **78:**31–37.
15. **Hung, S. L., P. L. Lee, H. W. Chen, L. K. Chen, C. L. Kao, and C. C. King.** 1999. Analysis of the steps involved in Dengue virus entry into host cells. Virology **257:**156–167.
16. **Jackson, T., A. Sharma, R. A. Ghazaleh, W. E. Blakemore, F. M. Ellard, D. L. Simmons, J. W. Newman, D. I. Stuart, and A. M. King.** 1997. Arginine-glycine-aspartic acid-specific binding by foot-and-mouth disease viruses to the purified integrin alpha(v)beta3 in vitro. J. Virol. **71:**8357–8361.
17. **Khromykh, A. A., and E. G. Westaway.** 1994. Completion of kunjin virus RNA sequence and recovery of an infectious RNA transcribed from stably cloned full-length cDNA. J. Virol. **68:**4580–4588.
18. **Kimura, T., S. W. Gollins, and J. S. Porterfield.** 1986. The effect of pH on the early interaction of West Nile virus with P388D1 cells. J. Gen. Virol. **67:**2423–2433.
19. **Kimura, T., J. Kimura-Kuroda, K. Nagashima, and K. Yasui.** 1994. Analysis of virus-cell binding characteristics on the determination of Japanese encephalitis virus susceptibility. Arch. Virol. **139:**239–251.
20. **Kinney, R. M., S. Butrapet, G. J. J. Chang, K. R. Tsuchiya, J. T. Roehrig, N. Bhamarapravati, and D. J. Gubler.** 1997. Construction of infectious cDNA clones for dengue 2 virus: strain 16681 and its attenuated vaccine derivative, strain PDK-53. Virology **230:**300–308.
21. **Klimstra, W. B., K. D. Ryman, and R. E. Johnston.** 1998. Adaptation of Sindbis virus to BHK cells selects for use of heparan sulfate as an attachment receptor. J. Virol. **72:**7357–7366.
22. **Kopecky, J., L. Grubhoffer, V. Kovar, L. Jindrak, and D. Vokurkova.** 1999. A putative host cell receptor for tick-borne encephalitis virus identified by anti-idiotypic antibodies and virus affinoblotting. Intervirology **42:**9–16.
23. **Lai, C.-J., B. Zhao, H. Hori, and M. Bray.** 1991. Infectious RNA transcribed from stably cloned full-length cDNA of dengue type 4 virus. Proc. Natl. Acad. Sci. USA **88:**5139–5143.

23a. **Lobigs, M.** 1987. Genotypic and phenotypic studies on natural isolates and laboratory-derived variants of flaviviruses. Ph.D. thesis, Australian National University, Canberra.

24. **Lobigs, M., I. D. Marshall, R. C. Weir, and L. Dalgarno.** 1988. Murray Valley encephalitis virus field strains from Australia and Papua New Guinea: studies on the sequence of the major envelope protein gene and virulence for mice. Virology **165:**245–255.
25. **Lobigs, M., R. Usha, A. Nestorowicz, I. D. Marshall, R. C. Weir, and L. Dalgarno.** 1990. Host cell selection of Murray Valley encephalitis virus variants altered at an RGD sequence in the envelope protein and in mouse virulence. Virology **176:**587–595.
26. **Mackow, E., Y. Makino, B. T. Zhao, Y. M. Zhang, L. Markoff, W. A. Buckler, M. Guiler, R. Chanock, and C. J. Lai.** 1987. The nucleotide sequence of dengue type 4 virus: analysis of genes coding for nonstructural proteins. Virology **159:**217–228.
27. **Maldov, D. G., G. G. Karganova, and A. V. Timofeev.** 1992. Tick-borne encephalitis virus interaction with the target cells. Arch. Virol. **127:**321–325.
28. **Mandl, C. W., M. Ecker, H. Holzmann, C. Kunz, and F. X. Heinz.** 1997. Infectious cDNA clones of tick-borne encephalitis virus European subtype prototypic strain Neudoerfl and high virulence strain Hypr. J. Gen. Virol. **78:**1049–1057.
29. **Mandl, C. W., F. X. Heinz, and C. Kunz.** 1988. Sequence of the structural proteins of tick-borne encephalitis virus (western subtype) and comparative analysis with other flaviviruses. Virology **166:**197–205.
30. **Mason, P. W., P. C. McAda, T. L. Mason, and M. J. Fournier.** 1987. Sequence of the dengue-1 virus genome in the region encoding the three structural proteins and the major nonstructural protein NS1. Virology **161:**262–267.
31. **McAda, P. C., P. W. Mason, C. S. Schmaljohn, J. M. Dalrymple, T. L. Mason, and M. J. Fournier.** 1987. Partial nucleotide sequence of the Japanese encephalitis virus genome. Virology **158:**348–360.
32. **Monath, T. P., C. B. Cropp, G. S. Bowen, G. E. Kemp, C. J. Mitchell, and J. J. Gardner.** 1980. Variation in virulence for mice and rhesus monkeys among St. Louis encephalitis virus strains of different origin. Am. J. Trop. Med. Hyg. **29:**948–962.
33. **Monath, T. P., and F. X. Heinz.** 1996. Flaviviruses, p. 961–1034. *In* B. N. Fields, D. M. Knipe, and P. M. Howley (ed.), Fields virology, 3rd ed., vol. 1. Lippincott-Raven Publishers, Philadelphia, Pa.
34. **Neff, S., D. Sa-Carvalho, E. Rieder, P. W. Mason, S. D. Blystone, E. J. Brown, and B. Baxt.** 1998. Foot-and-mouth disease virus virulent for cattle utilizes the integrin alpha(v)beta3 as its receptor. J. Virol. **72:**3587–3594.
35. **Putnak, J. R., N. Kanesa-Thasan, and B. L. Innis.** 1997. A putative cellular receptor for dengue viruses. Nat. Med. **3:**828–829.
36. **Ramos-Castaneda, J., J. L. Imbert, B. L. Barron, and C. Ramos.** 1997. A 65-kDa trypsin-sensible membrane cell protein as a possible receptor for dengue virus in cultured neuroblastoma cells. J. Neurovirol. **3:**435–440.
37. **Rey, F. A., F. X. Heinz, C. Mandl, C. Kunz, and S. C. Harrison.** 1995. The envelope glycoprotein from tick-borne encephalitis virus at 2 angstrom resolution. Nature **375:**291–298.
38. **Rice, C. M., A. Grakoui, R. Galler, and T. J. Chambers.** 1989. Transcription of infectious yellow fever RNA from full-length cDNA templates produced by in vitro ligation. New Biol. **1:**285–296.
39. **Rice, C. M., E. M. Lenches, S. R. Eddy, S. J. Shin, R. L. Sheets, and J. H. Strauss.** 1985. Nucleotide sequence of yellow fever virus: implications for flavivirus gene expression and evolution. Science **229:**726–733.
40. **Roivainen, M., L. Piirainen, T. Hovi, I. Virtanen, T. Riikonen, J. Heino, and T. Hyypia.** 1994. Entry of coxsackievirus A9 into host cells: specific interactions with alpha v beta 3 integrin, the vitronectin receptor. Virology **203:**357–365.
41. **Rostand, K. S., and J. D. Esko.** 1997. Microbial adherence to and invasion through proteoglycans. Infect. Immun. **65:**1–8.
42. **Ruoslahti, E., and M. D. Pierschbacher.** 1987. New perspectives in cell adhesion: RGD and integrins. Science **238:**491–497.
43. **Sa-Carvalho, D., E. Rieder, B. Baxt, R. Rodarte, A. Tanuri, and P. W. Mason.** 1997. Tissue culture adaptation of foot-and-mouth disease virus selects viruses that bind to heparin and are attenuated in cattle. J. Virol. **71:**5115–5123.
44. **Salas-Benito, J. S., and R. M. del Angel.** 1997. Identification of two surface proteins from C6/36 cells that bind dengue type 4 virus. J. Virol. **71:**7246–7252.
45. **Stocks, C. E., and M. Lobigs.** 1998. Signal peptidase cleavage at the flavivirus C-prM junction: dependence on the viral NS2B-3 protease for efficient processing requires determinants in C, the signal peptide, and prM. J. Virol. **72:**2141–2149.
46. **Sumiyoshi, H., C. H. Hoke, and D. W. Trent.** 1992. Infectious Japanese encephalitis virus RNA can be synthesized from in vitro-ligated cDNA templates. J. Virol. **66:**5425–5431.
47. **Trent, D. W., R. M. Kinney, B. J. Johnson, A. V. Vorndam, J. A. Grant, V. Deubel, C. M. Rice, and C. Hahn.** 1987. Partial nucleotide sequence of St. Louis encephalitis virus RNA: structural proteins, NS1, ns2a, and ns2b. Virology **156:**293–304.
48. **Tyler, K. L., and B. N. Fields.** 1996. Pathogenesis of viral infection, p. 173–218. *In* B. N. Fields, D. M. Knipe, and P. M. Howley (ed.), Fields virology, 3rd ed. Lippincott-Raven, Philadelphia, Pa.
49. **van der Most, R. G., J. Corver, and J. H. Strauss.** 1999. Mutagenesis of the RGD motif in the yellow fever virus 17D envelope protein. Virology **265:**83–95.